

Yrast spectroscopy of  $^{54}\text{Cr}$ M. Devlin,<sup>1,\*</sup> D. R. LaFosse,<sup>1,†</sup> F. Lerma,<sup>1</sup> D. Rudolph,<sup>2,3</sup> D. G. Sarantites,<sup>1</sup> and P. G. Thirolf<sup>2</sup><sup>1</sup>Chemistry Department, Washington University, St. Louis, Missouri 63130<sup>2</sup>Sektion Physik, Ludwig-Maximilians-Universität München, D-85748 Garching, Germany<sup>3</sup>Department of Physics, Lund University, S-22100 Lund, Sweden

(Received 27 August 1999; published 16 December 1999)

High-spin levels in the heaviest stable isotope of chromium were observed following the fusion-evaporation reaction  $^{12}\text{C}(^{48}\text{Ca}, \alpha 2n)^{54}\text{Cr}$  at a beam energy of 157 MeV, using the GAMMASPHERE and MICROBALL detector arrays. Numerous yrast and near yrast levels are reported, and previously assigned  $7^+$  and  $9^+$  levels are suggested to be  $5^+$  and  $7^+$ , respectively. The inferred level scheme is compared with shell model calculations.

PACS number(s): 23.20.Lv, 21.60.Cs, 27.40.+z, 29.30.Kv

Gamma-spectroscopic studies of nuclei in the  $fp$  shell have a long history, one that includes both a period of active interest and a subsequent period with fewer publications. Recently, however, new experimental and theoretical developments have made further progress possible. For example, on the theoretical side, interest in the structure of nuclei in the vicinity of the  $N=28$  shell closure has increased in recent years [1–4], as improved methods have become available and interest in the structure of neutron-rich nuclei in general has increased. Experimentally, fragmentation reactions have been used to study light  $N=28$  nuclei [5,6], and arrays of modern Ge detectors and channel selection devices have made fusion evaporation reactions an attractive method of studying yrast states in such nuclei [7,8]. One interesting case is  $^{54}\text{Cr}$ , the heaviest stable isotope of chromium, for which the most extensive yrast study is that by Nathan *et al.* [9]. Subsequent lifetime information was obtained by Stuchbery *et al.* [10], though no new levels were added. As a result, despite extensive knowledge of low-spin states in  $^{54}\text{Cr}$ , the ground band is known to spin  $J=10\hbar$ , and no other levels are identified above  $J=5\hbar$ , other than two levels tentatively assigned as  $J^\pi=7^+$  and  $9^+$  [11]. Nonetheless, these results and Coulomb excitation experiments clearly demonstrated that the mid- $f$  shell nucleus  $^{54}\text{Cr}$  possesses a rotationlike ground band, built on a mildly oblate configuration [12].

We present here new results on high-spin levels in  $^{54}\text{Cr}$ , populated in a heavy-ion fusion evaporation reaction. These results include a weakly populated extension of the ground band, and identify another high-spin band built on a  $5^+$  level which becomes yrast above spin  $10\hbar$ .

The reaction  $^{12}\text{C}(^{48}\text{Ca}, \alpha 2n)$  at 157 MeV was used to populate  $^{54}\text{Cr}$ . The target consisted of 0.10 mg/cm<sup>2</sup> of  $^{12}\text{C}$  with a 0.30 mg/cm<sup>2</sup>  $^{197}\text{Au}$  backing. The beam was accelerated by the 88 Inch Cyclotron at Lawrence Berkeley Na-

tional Laboratory. GAMMASPHERE [13] with 95 Ge detectors was used to detect  $\gamma$  rays, in coincidence with the MICROBALL [14], a  $4\pi$ , 95-element CsI detector array in which evaporated light charged particles were detected and identified. Events with at least three cleanly detected  $\gamma$  rays were recorded for off-line analysis. Due to the inverse kinematics of the reaction, the  $\alpha$  particle detection efficiency of the MICROBALL was less than 50%. Approximately 6% of the total number of events were in coincidence with 1  $\alpha$  particle, representing  $\approx 7$  million events. These data were taken in approximately four hours, with an average current of two particle-nanoamps of beam. The dominant channel in coincidence with one  $\alpha$  particle is the  $\alpha 2n$  channel  $^{54}\text{Cr}$ , though small amounts of both  $^{53}\text{Cr}$  and  $^{55}\text{Cr}$  were also observed. The linear momentum of the detected  $\alpha$  particle is used to partially reconstruct the residue momentum, improving the event-by-event Doppler shift correction; nonetheless, the large recoil velocity and (to a lesser extent) the undetected momentum component due to the evaporated neutrons result in  $\gamma$ -ray energy resolution of  $\approx 8$  keV FWHM at 1 MeV, somewhat worse than is typical for studies of this type with heavier or more proton-rich nuclei.

The data were sorted into an  $E_\gamma$ - $E_\gamma$  matrix, from which coincidence relationships were inferred. Figure 1 shows various gated  $\gamma$ -ray energy spectra from this reaction, all in coincidence with only one  $\alpha$  particle detected in the MICROBALL. Significant contaminants are leakthrough from the  $xn$  and  $pxn$  channels by accidental coincidence or misidentification of  $\alpha$  particles. Such contamination is readily removed with single  $\gamma$ -ray gates, and is not seen in these spectra. The resulting high-spin level scheme proposed for  $^{54}\text{Cr}$  is shown in Fig. 2 and is summarized in Table I. Angular correlation information of the observed  $\gamma$  rays is also shown in the form of directional correlation of oriented states (DCO) ratios, determined by  $R_{\text{DCO}} = [I_\gamma(\theta, 90^\circ)]/[I_\gamma(90^\circ, \theta)]$ , where  $I_\gamma(\theta_x, \theta_y)$  is the intensity of a transition at  $\gamma$ -ray angle  $x$ , gated on a stretched  $E2$  transition at angle  $y$ , with  $\langle \theta \rangle = 37.1^\circ, 139.3^\circ$ . Such ratios are expected to be approximately one for stretched  $E2$  and pure dipole  $\Delta I=0$  transitions, and 0.5 for stretched  $\Delta I=1$  transitions, if the mixing ratio is small.

\*Present address: LANSCE-3, Los Alamos National Laboratory, Los Alamos, NM 87545.

†Present address: Department of Physics and Astronomy, SUNY at Stony Brook, Stony Brook, NY 11794.

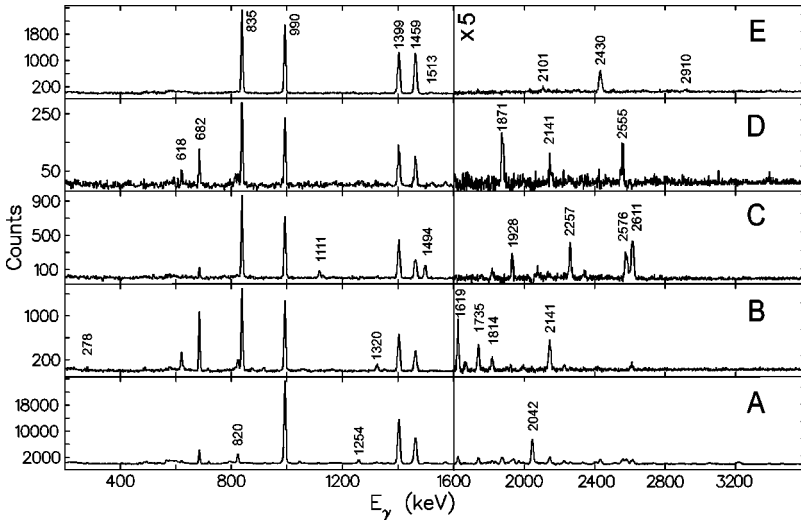


FIG. 1. Gamma-ray energy spectra in coincidence with the 835 keV (A), 1254 keV (B), 1567 keV (C), 1919 keV (D), and 2042 keV (E) transitions in  $^{54}\text{Cr}$  and one detected  $\alpha$  particle.

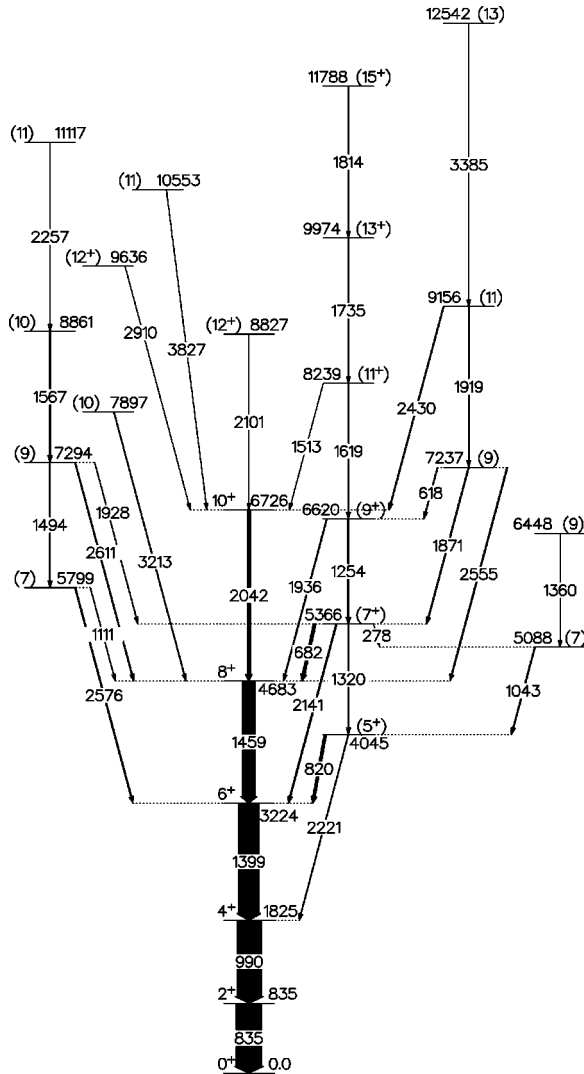


FIG. 2. High-spin level scheme for  $^{54}\text{Cr}$  deduced in the present work.

The ground band transitions up to  $10^+$  have been confirmed, though above this level the primary discrete feeding is via an apparent dipole transition at  $E_\gamma=2430$  keV. The yrast  $12^+ \rightarrow 10^+$  is identified as a 2101 keV transition. The shell model calculations of Saini and Gunye [15] anticipated that the yrast  $12^+$  would be at  $E_x=8.33$  MeV, while those of Horie and Ogawa [16] predicted 9.5 MeV. The present tentative placement of the yrast  $12^+$  at 8.8 MeV clearly agrees equally well with both calculations. The band built on the 4045 keV level has been extended to a tentative spin of  $(15^+)$ , and it is seen to become yrast above spin 10. Two other  $\gamma$ -ray sequences are observed, as seen in Fig. 2, and an additional five levels are indicated. Numerous known low-spin levels [11] are not observed, as is to be expected since this reaction populates  $^{54}\text{Cr}$  at higher spin, and nonyrast low-spin levels are by-passed in the subsequent decay.

The level at 4045 is strongly suggested to be a  $J=5$  state, rather than the tentative assignment of  $7^+$  given by Nathan *et al.* [9], based on the clear observation of a 2221 keV transition to the  $4^+$  level, and similar behavior at higher spin in this band. This assignment is in agreement with previous shell model calculations [15–18,10], which in general indicate an increased level density beginning at about 3.5 MeV, including the first  $5^+$  state. None of these calculations predict a  $7^+$  state at such a low energy. An example is the shell model calculation of McGrory [17], as presented in Watson *et al.* [19]. In these calculations, the lowest unnatural parity spin 3 and spin 5 states are predicted to occur between 3.5 and 4.0 MeV, while the lowest  $7^+$  is expected above 5 MeV. With the reassignment suggested here, the lowest  $5^+$  and  $7^+$  levels are at 4.04 and 5.36 MeV, respectively. The lowest observed  $J=3$  state is at 4128 keV [11], i.e., above the  $5^+$  level. This is consistent with it not being observed in the present work, if indeed it is positive parity. Note however that this  $J=3$ , 4128 keV level has been given both positive [11] and negative [19] parity assignments; therefore the energy of the first  $3^+$  state is an open question. The nonobservation of the 4045 keV level in the  $^{52}\text{Cr}(t,p)^{54}\text{Cr}$  work of Watson *et al.* [19] is also consistent with an unnatural parity

TABLE I. Level energies and  $\gamma$ -ray transition properties for the observed transitions in  $^{54}\text{Cr}$ . Tentative spin assignments are indicated by parantheses.

$E_x$ (keV)	$E_\gamma$ (keV)	$I_{\text{rel}}$ (%)	$R_{\text{DCO}}$	Assignment
835.3	835.3(3)	100	1.10(4)	$2^+ \rightarrow 0^+$ [9,10]
1824.9	989.6(3)	98(3)	0.97(4)	$4^+ \rightarrow 2^+$ [9,10]
3224.3	1399.4(4)	80(2)	0.96(4)	$6^+ \rightarrow 4^+$ [9,10]
4044.9	820.4(3)	9.2(3)	0.81(6)	$5^+ \rightarrow 6^+$
	2220.9(6)	1.7(1)	0.47(10)	$5^+ \rightarrow 4^+$
4683.4	1459.1(4)	51(2)	0.95(5)	$8^+ \rightarrow 6^+$ [9,10]
5087.6	1042.7(4)	2.8(1)	1.12(8)	$(7) \rightarrow 5^+$
5365.6	278.3(3)	0.29(3)		$7^+ \rightarrow (7)$
	682.3(3)	10(1)	0.90(6)	$7^+ \rightarrow 8^+$
	1319.9(5)	2.5(1)	0.86(9)	$7^+ \rightarrow 5^+$
	2141.3(6)	3.8(2)	0.88(8)	$7^+ \rightarrow 6^+$
5798.9	1110.9(4)	0.78(5)	0.96(12)	$(7) \rightarrow 8^+$
	2575.7(6)	3.4(1)	1.29(9)	$(7) \rightarrow 6^+$
6448.0	1360.4(4)	0.53(4)	1.31(12)	$(9) \rightarrow (7)$
6619.7	1254.2(4)	5.5(2)	1.04(7)	$9^+ \rightarrow 7^+$
	1936.0(5)	2.6(1)	1.33(9)	$9^+ \rightarrow 8^+$
6725.9	2042.5(5)	13(1)	0.98(6)	$10^+ \rightarrow 8^+$ [9,10]
7237.1	617.6(4)	1.8(1)	1.17(12)	$(9) \rightarrow 9^+$
	1870.5(5)	3.0(1)	1.35(8)	$(9) \rightarrow 7^+$
	2554.9(6)	3.2(1)	1.09(8)	$(9) \rightarrow 8^+$
7293.6	1494.3(4)	1.9(1)	1.05(9)	$(9) \rightarrow (7)$
	1927.9(5)	0.84(4)	1.27(12)	$(9) \rightarrow 7^+$
	2610.6(6)	2.7(1)	1.18(8)	$(9) \rightarrow 8^+$
7896.8	3213.4(8)	1.7(1)	1.38(9)	$(10) \rightarrow 8^+$
8238.8	1512.7(5)	0.38(3)		$(11^+) \rightarrow 10^+$
	1619.2(5)	2.6(1)	1.22(9)	$(11^+) \rightarrow 9^+$
8827.1	2101.2(6)	0.48(3)	0.9(1)	$(12^+) \rightarrow 10^+$
8860.6	1567.0(5)	3.1(1)	0.81(8)	$(10) \rightarrow (9)$
9156.1	1919.0(5)	1.1(1)	1.13(9)	$(11) \rightarrow (9)$
	2430.2(6)	2.7(1)	0.74(8)	$(11) \rightarrow 10^+$
9636.0	2910.2(7)	0.19(2)	1.13(20)	$(12^+) \rightarrow 10^+$
9973.6	1734.8(5)	1.6(1)	0.87(10)	$(13^+) \rightarrow (11^+)$
10533	3827.3(9)	0.18(2)	0.74(20)	$(11^+) \rightarrow 10^+$
11117	2256.7(6)	0.62(4)	0.69(10)	$(11) \rightarrow (10)$
11788	1814.1(5)	0.71(4)	0.99(11)	$(15^+) \rightarrow (13^+)$
12542	3385.4(9)	0.20(2)	1.1(2)	$(13) \rightarrow (11)$

assignment, as made here. Other shell model studies of  $^{54}\text{Cr}$  [10,15,16,18] also predict a cluster of  $1^+, 3^+, 5^+$  states around 3.5 to 4.0 MeV, though with somewhat varied energy orderings.

In order to further interpret these results, we have performed shell model calculations with the code RITSSCHIL [20] similar to those in Ref. [8], in which the calculations are compared with extensive data on nuclei near  $^{56}\text{Ni}$ . These modest calculations use a  $^{56}\text{Ni}$  core, and allow for the excitation of up to two particles across the  $N=Z=28$  shell gap. The  $^{54}\text{Cr}$  closed core involves two neutrons in the  $2p_{3/2}$ ,  $1f_{5/2}$ , and  $2p_{1/2}$  (upper  $fp$  shell) orbits, and two proton holes

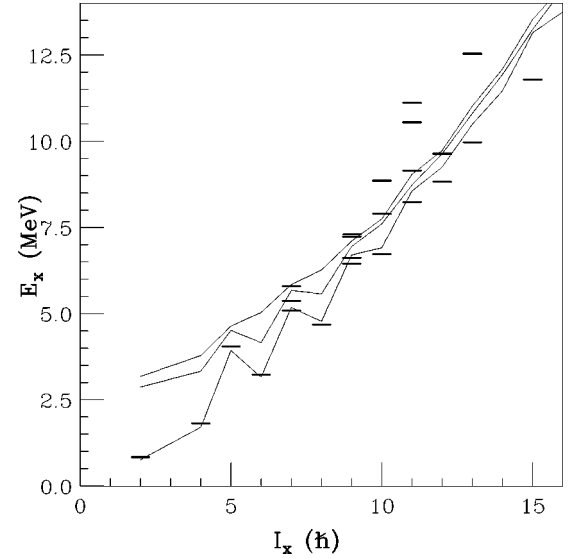


FIG. 3. Comparison of the shell model calculation for the lowest three levels (lines) of a given spin with the levels observed and assigned in the present work (horizontal bars) (see text).

in the  $1f_{7/2}$  shell. The FPD6 parameter set is used for the two-body residual interaction, and the single-particle energies are based on recent results from Trache *et al.* [21]. Details of the procedure can be found in Ref. [8].

The results of our calculations are similar to the ones described above. Figure 3 compares the predicted yrast and near-yrast positive parity states with the observed levels. The lines are drawn connecting the calculated yrast, first- and second-excited states as a function of spin; the levels assigned in the current experiment are shown as horizontal bars. Even in the moderate spin range ( $I=4-10\hbar$ ), the calculated levels agree with the observed levels, despite the relative distance from the assumed  $^{56}\text{Ni}$  core. Above  $\approx 12\hbar$  the limited shell model space of this calculation should become evident, and the lack of agreement there may reflect this. The position of the lowest  $7^+$  is similar to that in the earlier shell model calculations discussed above, and agrees well with the assignment made here.

Notably, the composition of the wave functions in the shell model calculation indicate that all of the levels are highly mixed, with typically no single component responsible for greater than 30% of any level. As a result, no dominant character can easily be assigned to any of the apparent rotational sequences observed. The apparent yrast structure above  $J=10$  presumably has at least a  $1p-1h$  composition, and is predicted to be composed primarily of neutron  $1p-1h$  states, with sizeable  $2p-2h$  admixtures. A full understanding of this structure will require a more sophisticated theoretical study.

The assistance of R. M. Clark, A. O. Macchiavelli, R. W. MacLeod, and I. Y. Lee in taking these data is gratefully acknowledged. This work was supported in part by the U.S. DOE under Grant No. DE-FG02-88ER-40406 (WU), and by the German BMBF under Project No. 06 LM 868.

- [1] J. Retamosa, E. Caurier, F. Nowacki, and A. Poves, *Phys. Rev. C* **55**, 1266 (1997).
- [2] B.A. Brown and W.A. Richter, *Phys. Rev. C* **58**, 2099 (1998).
- [3] A. Novoselsky, M. Vallières, and O. La'adan, *Phys. Rev. Lett.* **79**, 4341 (1997); A. Novoselsky and M. Vallières, *Phys. Rev. C* **57**, R19 (1998).
- [4] G.A. Lalazissis, D. Vretenar, P. Ring, M. Stoitsov, and L.M. Robledo, *Phys. Rev. C* **60**, 014310 (1999).
- [5] H. Scheit, T. Glasmacher, B.A. Brown, J.A. Brown, P.D. Cottle, P.G. Hansen, R. Harkewicz, M. Hellström, R.W. Ibbotson, J.K. Jewell, K.W. Kemper, D.J. Morrissey, M. Steiner, P. Thierolf, and M. Thoennessen, *Phys. Rev. Lett.* **77**, 3967 (1996).
- [6] T. Glasmacher, B.A. Brown, M.J. Chromik, P.D. Cottle, M. Fauerbach, R.W. Ibbotson, K.W. Kemper, D.J. Morrissey, H. Scheit, D.W. Sklenicka, and M. Steiner, *Phys. Lett. B* **395**, 163 (1997).
- [7] P.H. Regan, J.W. Arrison, U.J. Hüttmeier, and D.P. Balamuth, *Phys. Rev. C* **54**, 1084 (1996).
- [8] D. Rudolph, C. Baktash, M.J. Brinkman, M. Devlin, H.-Q. Jin, D.R. LaFosse, L.L. Riedinger, D.G. Sarantites, and C.-H. Yu, *Eur. Phys. J. A* **4**, 115 (1999).
- [9] A.M. Nathan, J.W. Olness, E.K. Warburton, and J.B. McGrory, *Phys. Rev. C* **17**, 1008 (1978).
- [10] A.E. Stuchbery, I. Morrison, D.L. Kennedy, and H.H. Bolotin, *Nucl. Phys.* **A337**, 1 (1980).
- [11] R.B. Firestone, *Table of Isotopes*, 8th ed. (Wiley New York, 1996).
- [12] C.W. Towsley, D. Cline, and R.N. Horoshko, *Nucl. Phys.* **A250**, 381 (1975).
- [13] I. Y. Lee, *Nucl. Phys.* **A520**, 641c (1990).
- [14] D.G. Sarantites, P.-F. Hua, M. Devlin, L.G. Sobotka, J. Elson, J.T. Hood, D.R. LaFosse, J.E. Sarantites, and M.R. Maier, *Nucl. Instrum. Methods Phys. Res. A* **381**, 418 (1996).
- [15] S. Saini and M.R. Gunye, *Phys. Rev. C* **24**, 1694 (1981).
- [16] H. Horie and K. Ogawa, *Nucl. Phys.* **A216**, 407 (1973).
- [17] J.B. McGrory, *Phys. Rev.* **160**, 915 (1967).
- [18] J. Vervier, *Nucl. Phys.* **78**, 497 (1966).
- [19] D.L. Watson, M.A. Abouzeid, H.T. Fortune, L.C. Bland, and J.B. McGrory, *Nucl. Phys.* **A406**, 291 (1983).
- [20] D. Zwarts, *Comput. Phys. Commun. A* **38**, 365 (1985).
- [21] L. Trache, A. Kolomiets, S. Shlomo, K. Heyde, H. Dejbakhsh, C.A. Gagliardi, R.E. Tribble, X.G. Zhou, V.E. Jacob, and A.M. Oros, *Phys. Rev. C* **54**, 2361 (1996).